

Triple Band Notched DG-CEBG Structure Based UWB MIMO/Diversity Antenna

Naveen Jaglan^{1, 2, *}, Samir D. Gupta¹, Binod K. Kanaujia³,
Shweta Srivastava¹, and Ekta Thakur²

Abstract—A MIMO/Diversity antenna with triple notch characteristics is proposed in this article. The proposed antenna has triple notches in the WiMAX band (3.3–3.6 GHz), WLAN band (5–6 GHz), and X-band satellite communication (7.2–8.4 GHz) band. Defected Ground Compact Electromagnetic Band Gap (DG-CEBG) is a design used to accomplish band notches. Defected ground planes are utilised so as to achieve compactness in conventional EBG structures. The proposed WiMAX band, WLAN band, and X-band satellite communication band DG-CEBG structures show a compactness of around 46%, 50%, and 48%, respectively, over a conventional EBG structure. In these structures, decoupling strips and a slotted ground plane are used to enhance the isolation between two closely spaced UWB monopoles. The individual monopoles are 90° angularly separated with a stepped structure which helps to reduce mutual coupling and also contributes towards impedance matching by increasing the current path length. $|S_{21}|$ or mutual coupling is found to be less than 15 dB over the whole UWB frequency range. The Envelope Correlation Coefficient (≤ 0.5) is within the acceptable limits over the whole UWB frequency range. Notched frequency depends on the parameters of DG-CEBG structures; when there is a change in these parameters notch frequency is also changed. A low cost FR-4 substrate with thickness (h) = 1.6 mm, permittivity (ϵ) = 4.4 and loss tangent (δ) = 0.02 is used for the proposed antenna, and it has a compact size of $58 \times 45 \times 1.6$ mm³.

1. INTRODUCTION

Since 2002, when Federal communications Commission (FCC) unconstrained the UWB [1] spectrum (3.1–10.6 GHz) for unconstrained commercial uses, there has been frequent need of UWB antennas. Circular monopoles [2] are the ideal model for UWB applications owing to advantages such as simplicity of production, satisfactory radiation characteristics, and huge impedance bandwidth. However, some applications such as those operating in the WLAN (5–6 GHz), WiMAX (3.3–3.6 GHz), and X-band satellite communication band (7.2–8.4 GHz) cause interference problems in the UWB frequency range. To avoid such interferences, an antenna with multiband rejection is required.

A number of approaches have been described in the literature for achieving triple band notch designs. Notches for WiMAX, WLAN, and the X-band satellite communication band frequencies are achieved by etching two elliptic single complementary split-ring resonators (ESCSRRs) of dissimilar dimensions [3] in the patch and split-ring resonators joining the feed-patch connection of the antenna. The band-rejection characteristics can be achieved by introducing the band reject elements [4] in the feed line of the UWB antenna. A multi-band antenna [5] can be made by using numerous fine strips

Received 7 September 2017, Accepted 10 November 2017, Scheduled 1 December 2017

* Corresponding author: Naveen Jaglan (naveenjaglan1@gmail.com).

¹ Department of Electronics & Communication Engineering, Jaypee Institute of Information Technology, Noida, Uttar Pradesh, India. ² Department of Electronics & Communication Engineering, Jaypee University of Information Technology, Waknaghat, Solan, Himachal Pradesh, India. ³ School of Computational & Integrative Sciences, Jawaharlal Nehru University (J.N.U.), New Delhi 110067, India.

behaving as resonance tracks unified with a DSP (diamond-shaped patch) antenna. Adding Hook-type defected ground structure (DGS) on ground plane, or inserting Ω -type slot on the radiator [6] and adding a semi-octagon-type resonant ring on the patch of the antenna can give triple notched frequency bands. To produce triple band-notched feature, three open-ended quarter-wavelength slots are used [7]. A conventional slot with open-ends and a quarter-wavelength is engraved in the radiator, and three half-wavelength semi-circular slots are cut in the radiator to produce the triple band rejection antenna in [8]. Expending analogous ideas for triple notched antennas are suggested by different authors in [9–12]. In [13] a triple band rejection notched antenna using electric ring resonator is shown. In [14], a triple band notch antenna using a hollow cross-loop resonator is shown. In [15], a triple band notch antenna using particle swarm optimisation and firefly algorithm is shown. In [16], slots are made on the microstrip feed line to obtain triple band notch characteristics. In [17], a triple band notched antenna using slots in the radiators is shown. In [18], a triple band notched antenna is obtained using C-shaped slots in the radiator and ground plane. In [19], a triple band notched antenna is obtained using an arc-shaped slot in the radiator and a U-shaped slot in the ground plane. Problem with these approaches is that all approaches are antenna design specific and give poor control on notch location and width. These approaches of obtaining notches are totally dependent on the antenna shape, and one method of notch creation may not be suitable for another antenna design. Moreover, the UWB antenna with single or double notches is obtained using EBG structures but in WLAN band only. The authors of [20] make use of four EBG structures in [20, 21] to achieve one notch.

A multiple-input–multiple-output (MIMO)/Diversity communication system requires the use of multiple antennas employed at the transmitter and/or receiver with low mutual coupling between them. MIMO communication system achieves enhancement in the data rate in multipath signal propagation. The MIMO technology used in UWB will provide an increase in channel capacity over that used in a narrowband system [22]. UWB MIMO system behaviour is considered in [23–25]. However, when MIMO systems are employed for compact portable devices, the high electromagnetic coupling among antennas affects system behaviour significantly [26, 27]. Different techniques are used to decrease mutual coupling between antenna elements, such as novel antenna designs [28, 29], using slots in the ground plane [30–32] and use of EBG patches [33, 34]. The designs in [35–37] are not capable of functioning over the complete band unrestricted by FCC.

MIMO antennas with band-rejection characteristics have been investigated by various researchers [38–42]. In [43], a parasitic strip and open ended slots are used to obtain a dual band notched MIMO antenna. In [44], a WLAN band-notched two-element G-shaped antenna is shown. A majority of these designs form the notches by altering the radiators. In [45], MIMO antennas with band rejection features were considered without modifying the antenna patch but restrained intervention from the WLAN systems only.

In the proposed antenna, a MIMO system composed of two 90° angularly separated semi-circular stepped monopoles with a decoupling network for UWB applications is proposed. The slotted ground plane and decoupling strips are used to reduce the electromagnetic coupling among the elements. Stepped UWB monopole antennas are employed with DG-CEBG structures to acquire triple band notches in WiMAX, WLAN, and X-band satellite communication bands. This method of notch generation is formula based and independent of the antenna design. The consequences of altering the DG-CEBG structure parameters on notched frequencies are also explained.

2. SELECTIVE BAND GAP CREATION BY MEANS OF EBG STRUCTURES FOR CIRCULATING SURFACE WAVES

Mushroom electromagnetic bandgap designs are a type of frequency selective surface. These designs operate as band rejection filters in explicit frequency bands and also offer very high impedance, consequently specified as a high impedance surface [46–51]. Mushroom EBGs are made up of conducting patches and shorted vias that connect patches with ground planes. These EBG structures act as LC filters where L is due to the current flow through via and C owing to the gap between patches. The important equations used for designing mushroom EBG structures are given below [46].

$$L = 0.2h \left[\ln \left(\frac{2h}{r} \right) - 0.75 \right] \quad (1)$$

$$C = \epsilon_0 \epsilon_r \frac{W^2}{h} \tag{2}$$

$$\omega_0 = \frac{1}{\sqrt{LC}} \tag{3}$$

where, L and C describe the inductance and capacitance, respectively. W is the width of the EBG patch, ϵ_r the relative permittivity, ϵ_0 the absolute permittivity, ω_0 the resonant frequency, h the via height, and r the radius of mushroom structures.

3. GRADUAL BUILD-OUT OF PROPOSED MIMO/DIVERSITY ANTENNA DESIGN

A UWB planar antenna structure is considered as a basic design in this paper, and only unit cells of the DG-CEBG are positioned in the neighbourhood of microstrip feed of the basic antenna design. The proposed DG-CEBG structures consist of spiral shaped slots in the top and bottom planes of the conventional EBG structures. This increases the total inductance of the equivalent circuit thereby making the structures more compact. If one interfering scheme is active in the UWB functioning range at a time, then only a single notch is essential. Therefore, a single DG-CEBG element can be placed close to the microstrip feed to achieve the desired notch. When disturbance is from the WiMAX band (3.3–3.6 GHz), WLAN band (5–6 GHz), and the X-band satellite communication (7.2–8.4 GHz) band, then three EBG designs are essential to reject these bands. The smallest DG-CEBG design is accountable for the notch in the X-band satellite communication band.

Expansion of the proposed UWB MIMO/Diversity antenna with triple band notches by means of DG-CEBG cells is revealed in Figure 1. Antenna 3 demonstrates the improved perimeter of the radiator.

$$f_r = \frac{1}{2\pi \sqrt{(L_1 + L_2 + L_3)(C_1 + C_0)}} \tag{4}$$

The increase in the current path length helps to accomplish proper impedance matching [52] and improves partition among individual antennas. Antenna 4 uses the DG-CEBG structure to obtain triple band notches. Antenna 6 is shown with triple band notches and the decoupling strips to decrease mutual coupling among individual antennas. A variety of intermediary antenna structures are also shown, which are used intermediately in realizing the proposed antenna 6 structure. Figure 2 shows the development of the DG-CEBG structure from conventional mushroom EBG structure. Figure 3 shows

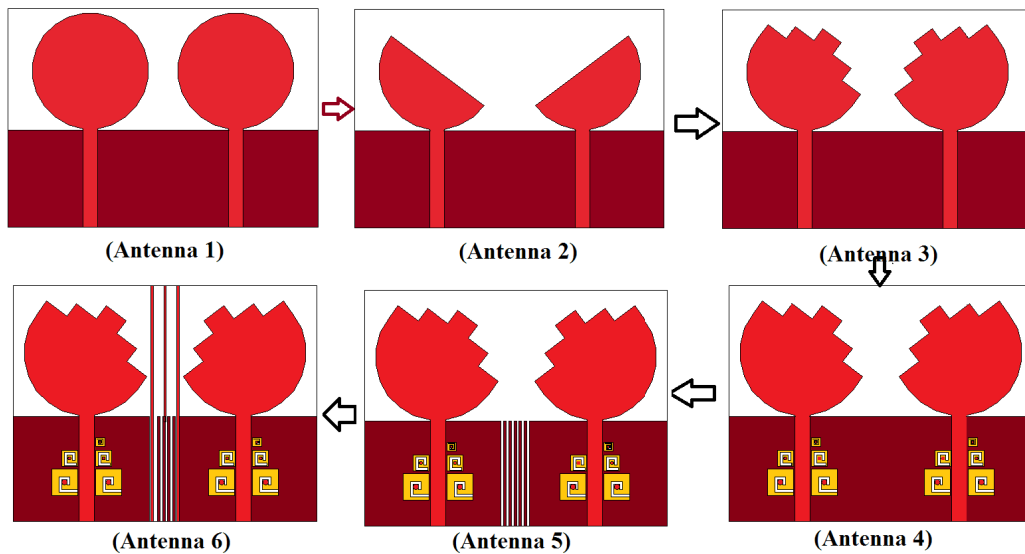


Figure 1. Stepwise expansion of the triple notched MIMO/Diversity antenna.

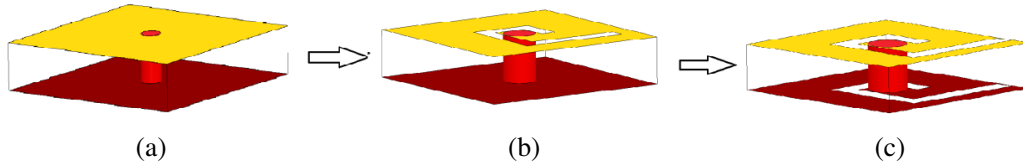


Figure 2. Development of the DG-CEBG structure from the mushroom EBG structure.

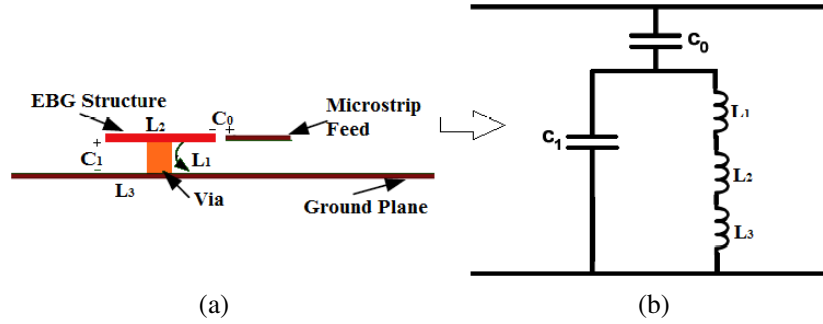


Figure 3. (a) A DG-CEBG structure placed near the antenna feed; (b) Equivalent circuit of (a).

the equivalent circuit of DG-CEBG cell, and Equation (4) gives the resonant frequency. L_2 and L_3 show the inductance in series due to spiral-shaped slots in the top and bottom planes of conventional EBG structures.

4. PROPOSED UWB MIMO/DIVERSITY ANTENNA WITH TRIPLE NOTCHES

Figure 4 illustrates the geometry of a sample UWB antenna with DG-CEBG design cells. The antenna design parameters are shown in Table 1. The simulated current distribution of the proposed antenna is shown in Figure 5 for additional examination. It may be seen straightforwardly in Figure 5 that dissimilar DG-CEBG designs have different current circulations at dissimilar frequencies with the highest current in their bandgaps. Figure 6 demonstrates the made-up prototype of the proposed antenna. The simulation is performed using Ansoft HFSS v.14. The proposed antenna has a VSWR which is calculated by means of AgilentTM Network Analyzer PNA-L series.

5. RESULTS

The VSWR variations of all intermediate antennas along with the proposed antenna are shown in Figure 7. It is verified that each DG-CEBG cell is responsible for notch generation in its band. The radiation principle of the antenna is also implicit from Figure 7 because in the DG-CEBG [53] band gap ($VSWR > 2$), total input power does not get transferred to the antenna, and as such, no radiation takes place. The VSWRs of antennas 1 and 3 are close to each other because the perimeters of antenna 1 and 3 are the same. In antenna 4 and antenna 5, steps are taken to reduce the mutual coupling, which will not have any effect on notched frequencies. So, antennas 4 and 5 have notched frequencies close to each other.

The antenna design parameters of the proposed antenna shown in Table 1 are calculated and optimized experimentally. Figure 8 shows the simulated $|S_{21}|$ (mutual coupling) between the two participating ports of the different antennas.

As mutual coupling of less than 15 dB is enough for most of the UWB applications, the antenna is appropriate for MIMO/Diversity purpose over the whole UWB. Figure 8 also illustrates the mutual coupling between antenna 6 and antenna 1, antenna 2 and antenna 3, antenna 4 and antenna 5. When Port 1 of the proposed antenna is energized, the current from the patch has a tendency to couple to Port 2. This is blocked by the decoupling arrangement consequently reducing the wide-band electromagnetic

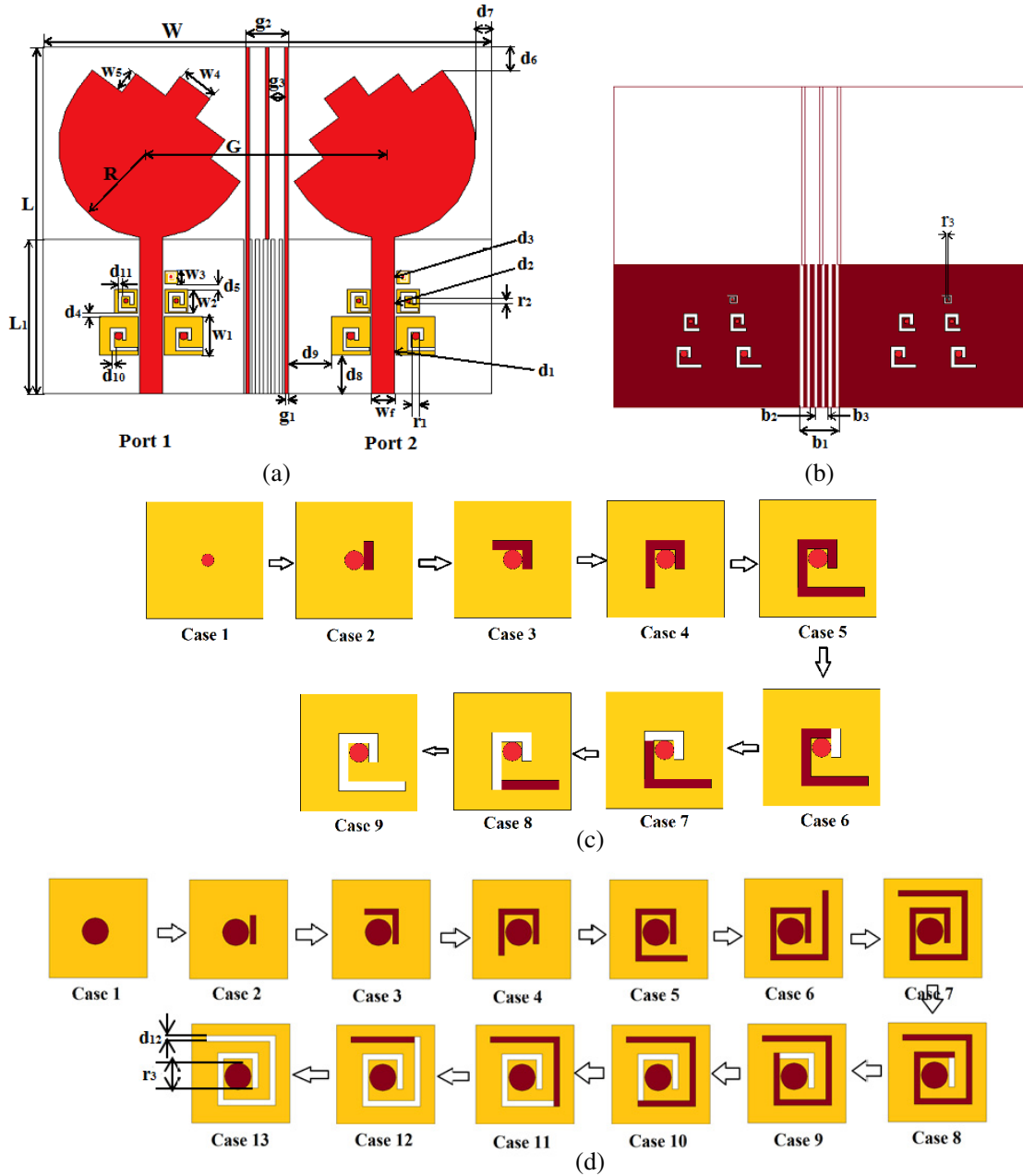


Figure 4. (a) Upper view. (b) Back view of proposed antenna. (c) Upper view of WiMAX and WLAN DG-CEBG structures. (d) Top view of X-band satellite communication band DG-CEBG structure (Antenna 6).

coupling. The result is identical when Port 2 of antenna 6 is energized. It is seen that the isolation of the proposed antenna can be improved by decoupling among the radiators across the whole UWB without disturbing the notched frequencies. Figure 9 illustrates the simulated and measured VSWRs of antenna 6. The notch in the WiMAX band has its midpoint at 3.4 GHz with a simulated VSWR magnitude of 5.2 and measured VSWR magnitude of 4.7. The notch in the WLAN band has its midpoint at 5.5 GHz with a simulated VSWR magnitude of 6.1 and measured VSWR magnitude of 5.6. The midpoint of the notch in X-band satellite communication band is at 7.6 GHz with a simulated VSWR magnitude of 5.1 and measured VSWR magnitude of 4.6. Figure 10 shows that the simulated and measured

Table 1. Antenna design parameters of the proposed antenna (antenna 6).

Parameters	Value (mm)
Circular disc monopole radius (r)	12
Length of antenna ground plane (L_1)	20
Width of antenna Substrate (W)	58
Length of antenna Substrate (L)	45
Width of antenna microstrip feed (W_f)	3
Space among ground and circular disc (h)	0.3
Radius of via of WiMAX DG-CEBG structures (r_1)	0.5
Radius of via of WLAN DG-CEBG structures (r_2)	0.3
Radius of via of 7.2–8.4 GHz band DG-CEBG (r_3)	0.25
Space between antenna feed and WiMAX EBG (d_1)	0.2
Space among WiMAX DG-CEBG & WLAN DG-CEBG (d_4)	0.52
Space among WLAN DG-CEBG & 7.2–8.4 GHz DG-CEBG (d_5)	0.78
Space amid two monopole antennas (G)	30
Spacelinking feed line and 7.2–8.4 GHz band DG-CEBG (d_3)	0.25
Space between feed line and WLAN DG-CEBG (d_2)	0.25
Decoupling structure strip width (g_1)	0.5
Space between decoupling elements (g_3)	2.5
Space between decoupling elements (g_2)	5.5
Space on the top of elements (d_6)	2.96
Space on the side of elements (d_7)	2
Step width on semi-circular monopole (W_4)	4.8
Step height on semi-circular monopole (W_5)	3.07
Space between WiMAX DG-CEBG and decoupling element (d_9)	0.75
Space between WiMAX DG-CEBG and antenna feed (d_8)	5
Width of slot in ground plane (b_3)	0.5
Space between slots in ground plane (b_2)	0.5
Slotted ground plane width (b_1)	5.5
Edge length of DG-CEBG for WiMAX notch (W_1)	5
Edge length of DG-CEBG for WLAN notch (W_2)	3
Edge length of DG-CEBG for 7.2–8.4 GHz band notch (W_3)	1.7
Slot width on WiMAX DG-CEBG structure (d_{10})	0.5
Slot width on WLAN DG-CEBG structure (d_{11})	0.5
Slot width on 7.2–8.4 band DG-CEBG structure (d_{12})	0.1

values of mutual coupling ($|S_{21}|$) in the proposed antenna are well below 15 dB over the whole UWB frequency range. Figure 10 also illustrates that simulated and measured magnitudes of $|S_{21}|$ are in fairly good agreement for antenna 6. The electromagnetic interaction between the antenna elements causes mutual coupling in antennas. Figure 11 illustrates that antennas with single DG-CEBG designs have lower VSWR magnitudes at WiMAX and WLAN notched frequencies than the antennas with double DG-CEBGs. Figure 12 illustrates the consequence of stepwise inductance enhancement when only one WiMAX DG-CEBG cell is placed in antenna 6. Case 1 to Case 9 layouts of WiMAX DG-CEBG cell are shown in Figure 4(c). Maximum inductance is observed in case 9, and therefore the notched frequency

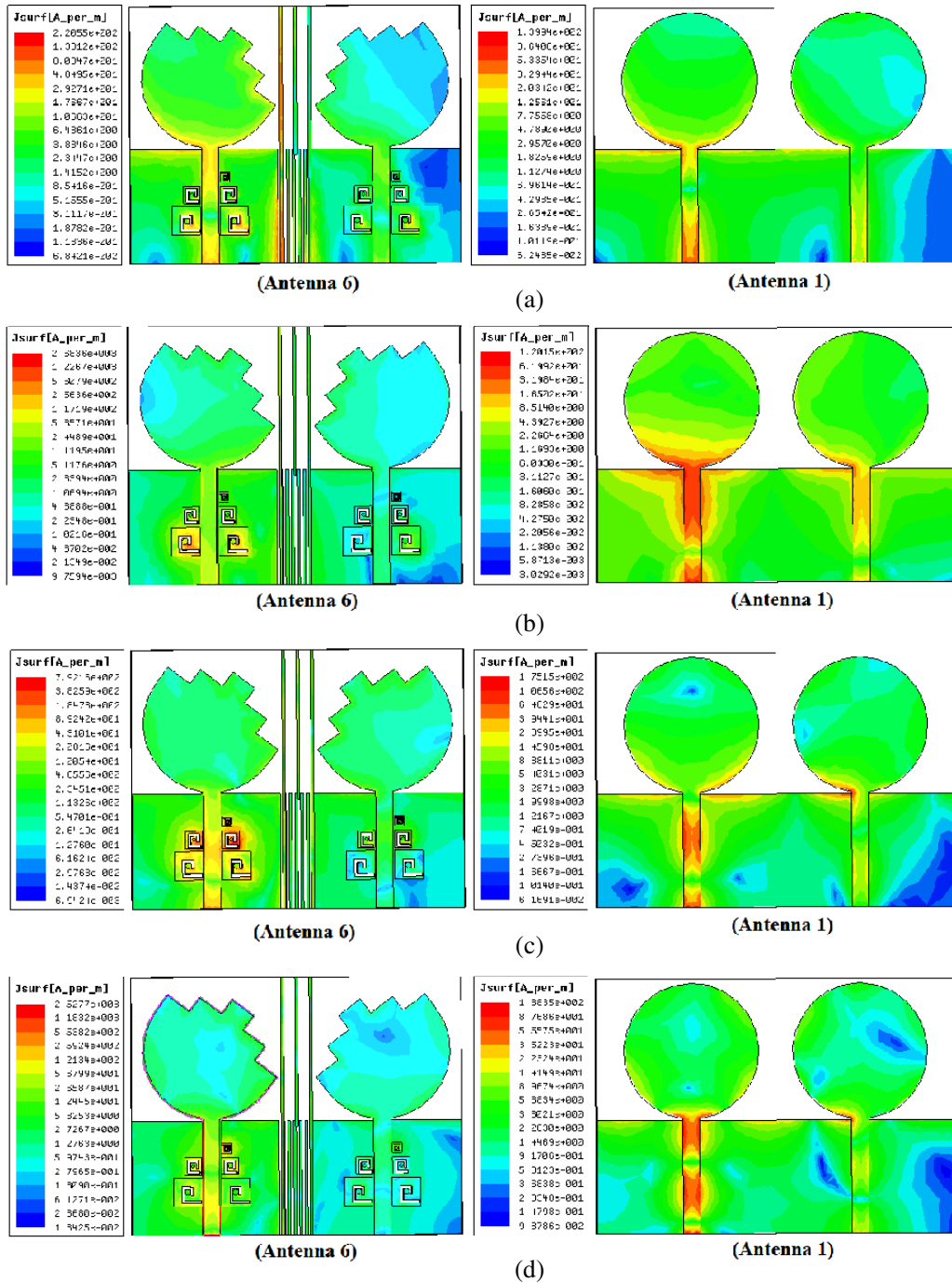


Figure 5. Surface current circulation of the proposed triple band antenna at notched frequencies of (a) 3.1 GHz, (b) 3.4 GHz, (c) 5.5 GHz, and (d) 7.5 GHz.

in this case is minimum. Similarly, Figure 13 shows the effect of inductance enhancement when only one WLAN DG-CEBG cell is used in antenna 6. The maximum inductance in WLAN DG-CEBG cell is corresponding to case 9 layout of Figure 4(c). Figure 14 shows the incremental inductance effect when only the 7.2 GHz–8.4 GHz band DG-CEBG structure is used in antenna 6. From case 1 to case 13, inductance is increased because of the increase in spiral turns. The top views of case 1 to case 13 DG-CEBG cells giving the total number of turns are shown in Figure 4(d).

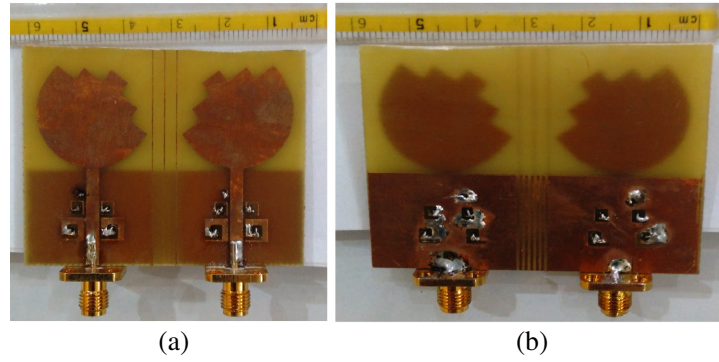


Figure 6. (a) Front view. (b) Back view of the fabricated triple band rejection antenna.

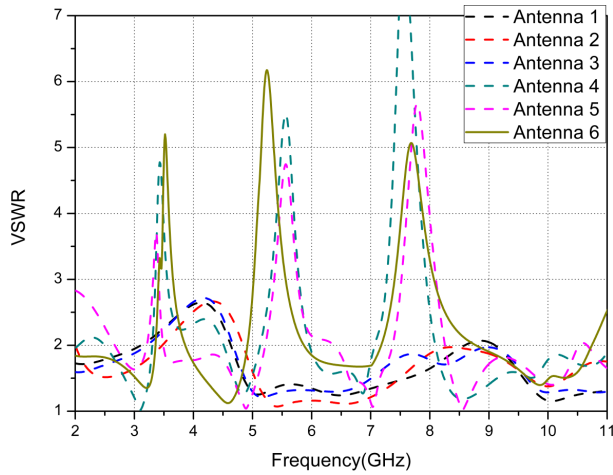


Figure 7. VSWR variation of the different antennas along with the proposed antenna.

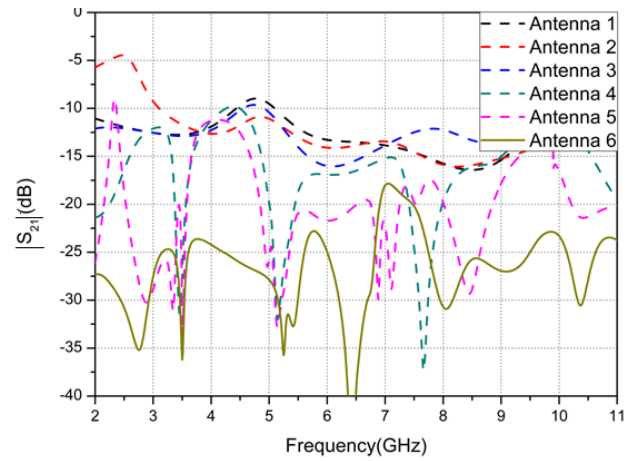


Figure 8. Mutual coupling in dissimilar antennas along with proposed antenna.

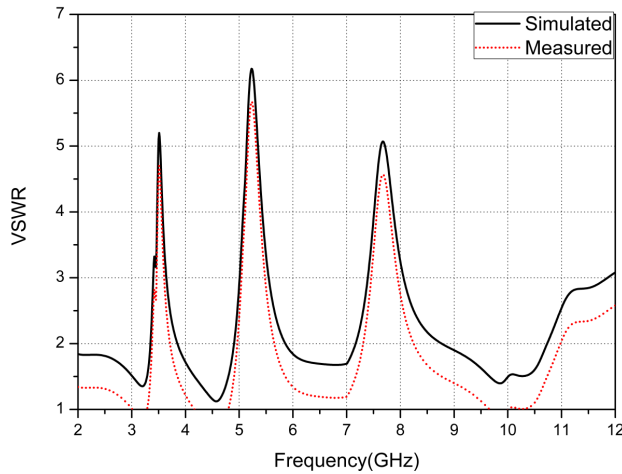


Figure 9. Simulated and measured VSWR of the proposed antenna.

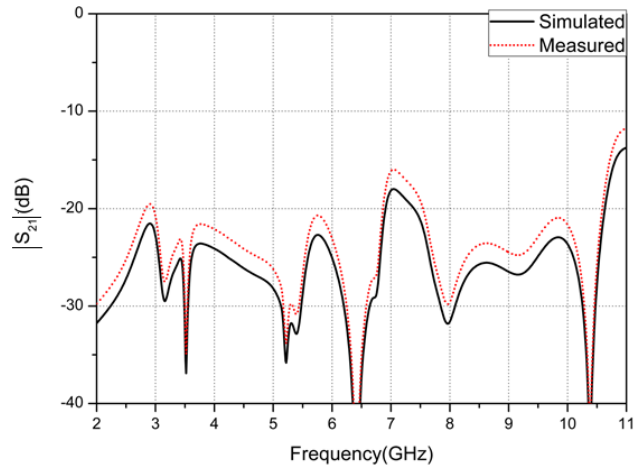


Figure 10. Variation of the simulated and measured mutual coupling ($|S_{21}|$).

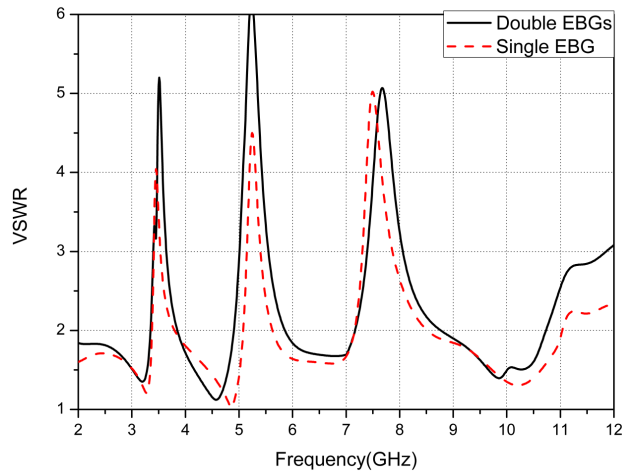


Figure 11. Simulated VSWR when EBGs are placed at single and double side of feed.

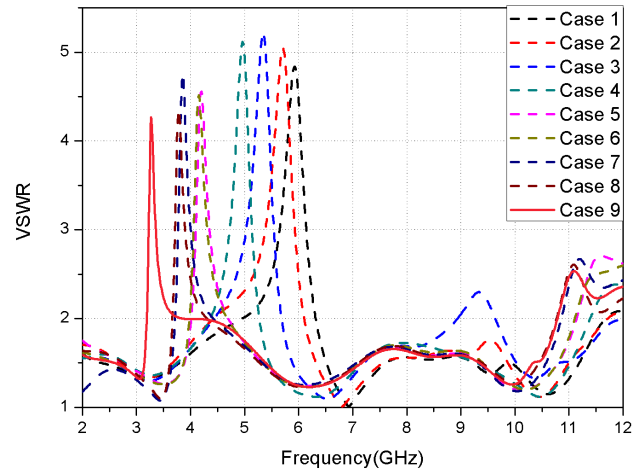


Figure 12. Reduction of notch frequencies in the WiMAX band with incremental inductance.

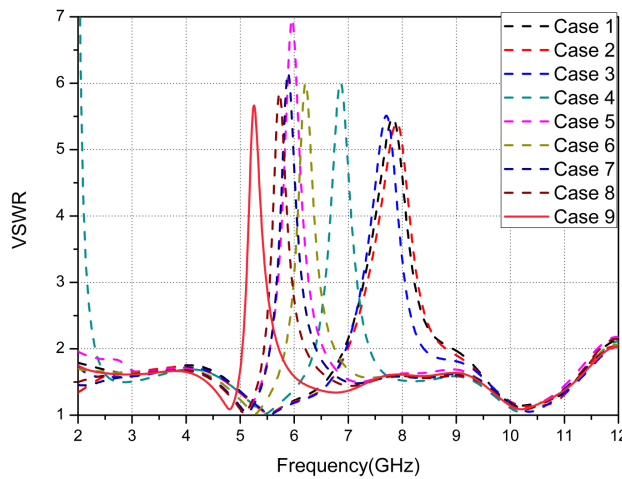


Figure 13. Reduction of notch frequencies in the WLAN band with incremental inductance.

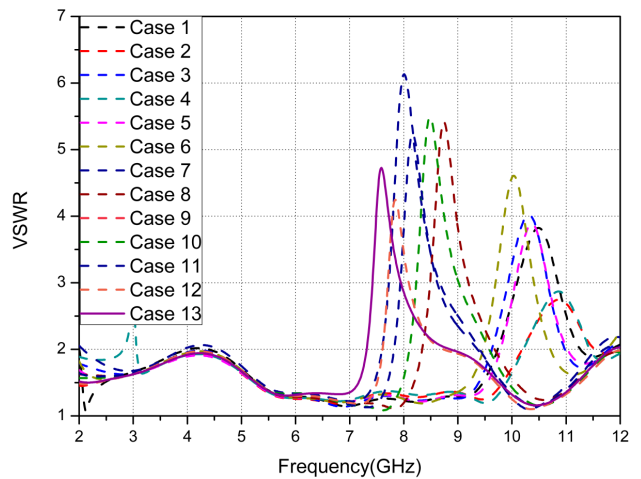


Figure 14. Reduction of notch frequencies in the 7.2 GHz–8.4 GHz band with incremental inductance.

Figure 15, Figure 16, and Figure 17 show the variation of VSWR with variations of the edge length of DG-CEBG structure which is used for WiMAX, WLAN and X-band satellite communication band-notch generation.

It can be seen that increasing W_1 , W_2 , and W_3 , all have the same effect of increasing the capacitance, and hence decreasing the resonant frequency as given by Equation (4).

Figure 18 shows the variation in VSWR when d_1 , i.e., space between the WiMAX DG-CEBG cell and the microstrip feed, is varied. Figure 19 reveals the variation in VSWR when d_2 , i.e., space between the WLAN DG-CEBG cell and the microstrip feed, is varied. Figure 20 reveals the variation in VSWR when d_3 , i.e., space between the 7.2 GHz–8.4 GHz DG-CEBG cell and the microstrip feed, is varied.

It is observed that a strong notched band is obtained if the space or the mutual coupling between the microstrip feed and DG-CEBG structures is decreased. There are minor variations in notched frequencies of other bands when the DG-CEBG cell corresponding to a specific band is moved. This is due to mutual coupling among the three DG-CEBG cells. Each DG-CEBG cell controls the notch frequency tuning of its own band. Figure 21 shows the variation of VSWR with the via radius of WiMAX

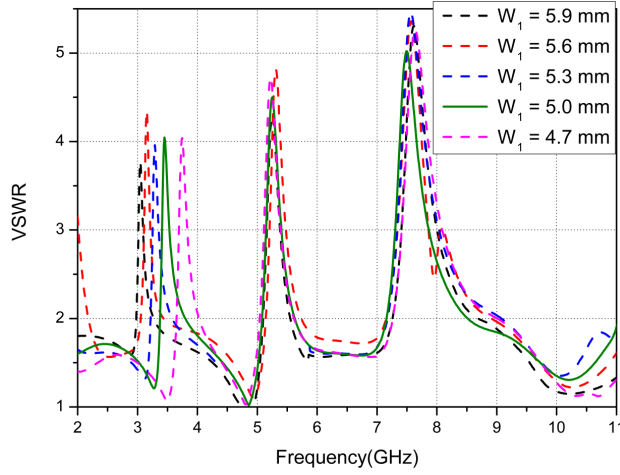


Figure 15. Variation of VSWR with the width (W_1) of the mushroom WiMAX DG-CEBG structure.

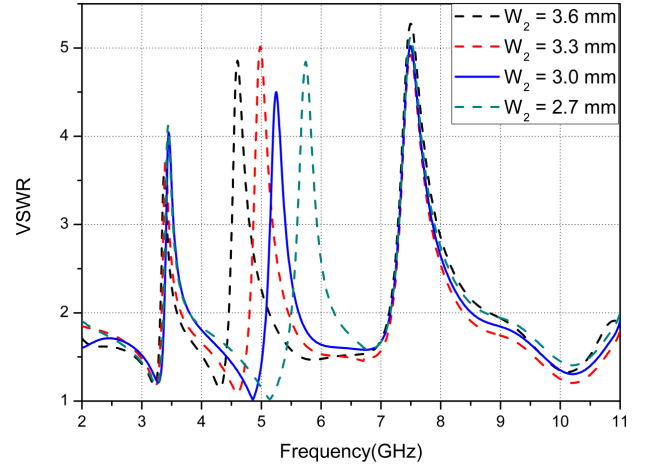


Figure 16. Variation of VSWR with the width (W_2) of the WLAN DG-CEBG structure.

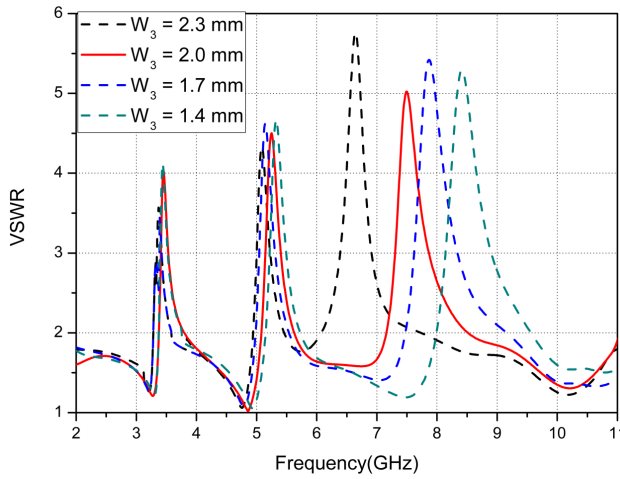


Figure 17. Variation of VSWR with the width (W_3) of 7.2 GHz–8.4 GHz band DG-CEBG structure.

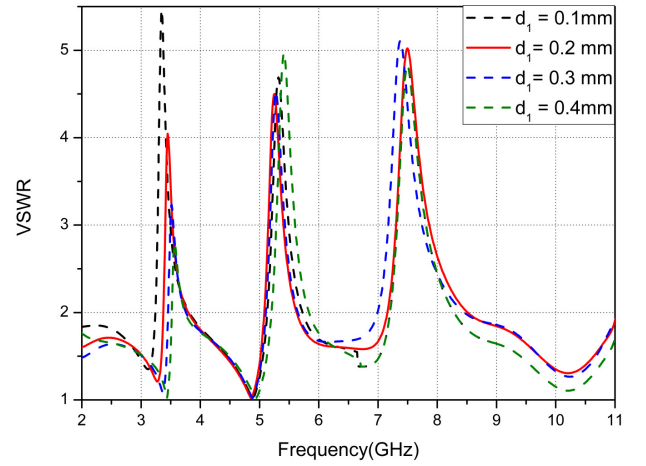


Figure 18. Variation of VSWR with the space (d_1) between the microstrip line and the WiMAX DG-CEBG structure.

and WLAN DG-CEBG structures. This can be easily verified using Equation (1) and Equation (4). As the radius of via (r) decreases, the inductance (L) given in Equation (1) increases thereby decreasing the resonant frequency (f_r) given in Equation (4). The antenna gain may be increased remarkably using a high impedance surface reflector [54, 55]. Furthermore, this reflector also helps in minimising back lobes, and increasing the front-back ratio DG-CEBG structures can also be used to make antenna operate in WLAN and WiMAX bands as done by the researchers in [56].

Figure 22 shows the radiation patterns of the proposed antenna at 4 GHz. Figure 22(a) shows E -plane co-polar and cross-polar radiation patterns for both simulated and measured values while Figure 22(b) shows H -plane co-polar and cross-polar radiation patterns for both measured and simulated values. Figure 23 shows the radiation patterns of the proposed antenna at 9 GHz. Figure 23(a) shows E -plane co-polar and cross-polar radiation patterns for both simulated and measured values while Figure 23(b) shows the H -plane co-polar and cross-polar radiation patterns for both measured and simulated values.

An antenna test kit is used to measure antenna radiation patterns, and a horn antenna is used as

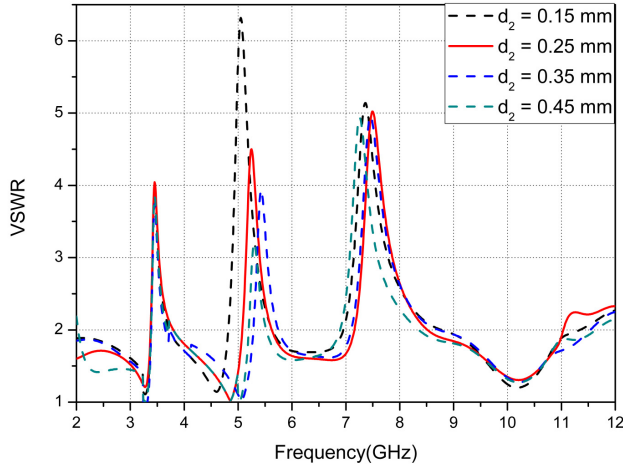


Figure 19. Variation of VSWR with the space between the microstrip line and WLAN DG-CEBG structure.

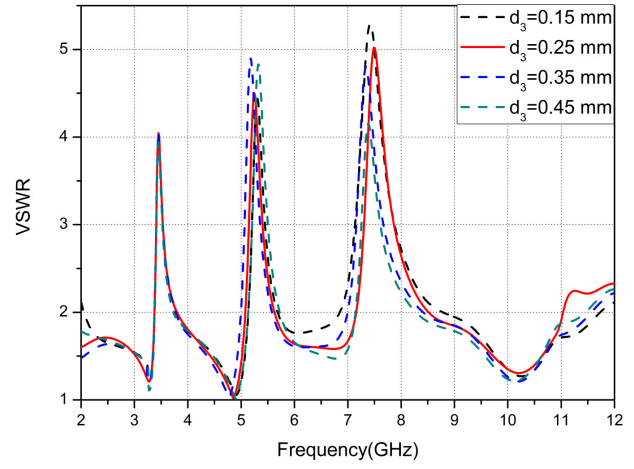


Figure 20. Variation of VSWR with the space between the microstrip line and WiMAX DG-CEBG structure.

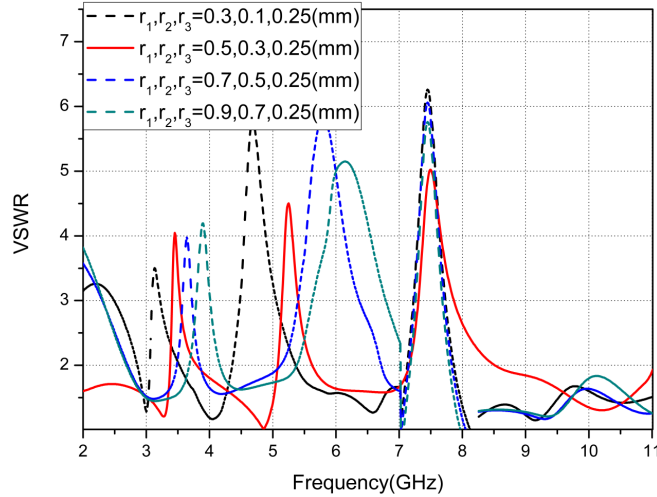


Figure 21. Variation of VSWR with the via radius of WiMAX and WLAN DG-CEBG structures.

the source which is placed at a proper distance from the test antenna. To obtain radiation patterns, port 1 or 2 of antenna 6 is excited while the other port is terminated with a $50\ \Omega$ load. Figure 24 shows that gain of the antenna decreases at the notched frequencies of WiMAX and WLAN bands. The two-port Envelope Correlation Coefficient (ECC) is an extremely important factor in antennas for MIMO applications. The ECC formula is given in Equation (5). The radiation efficiency of individual antennas is around 80% over the whole UWB frequency range.

The ECC (ρ_e) can be calculated with the technique discussed in [57, 58].

$$\rho_e = |\rho_{i,j}|^2 = \frac{|S_{ii}^* S_{ij} + S_{ji}^* S_{jj}|^2}{(1 - |S_{ii}|^2 - |S_{ji}|^2)(1 - |S_{jj}|^2 - |S_{ij}|^2) \eta_{rad,i} \eta_{rad,j}} \quad (5)$$

where $\eta_{rad,i}$ is the radiation efficiency of i -th antenna element.

Figure 25 shows the simulated and measured Envelope Correlation Coefficients (ρ_e) of the notched UWB MIMO/diversity antenna. Envelope Correlation Coefficient is below 0.01 over nearly the whole

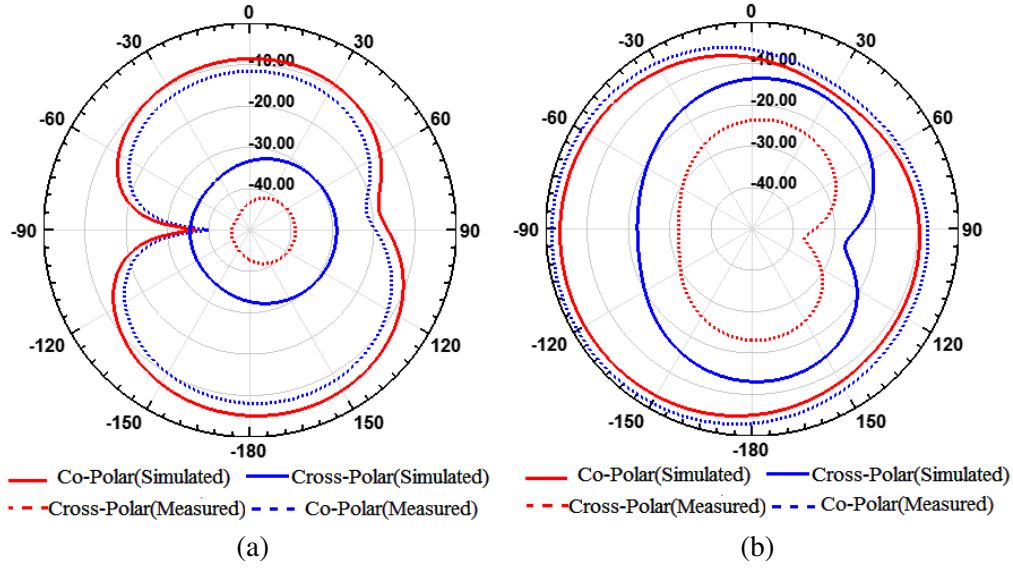


Figure 22. Radiation patterns at 4 GHz. (a) *E*-plane. (b) *H*-plane.

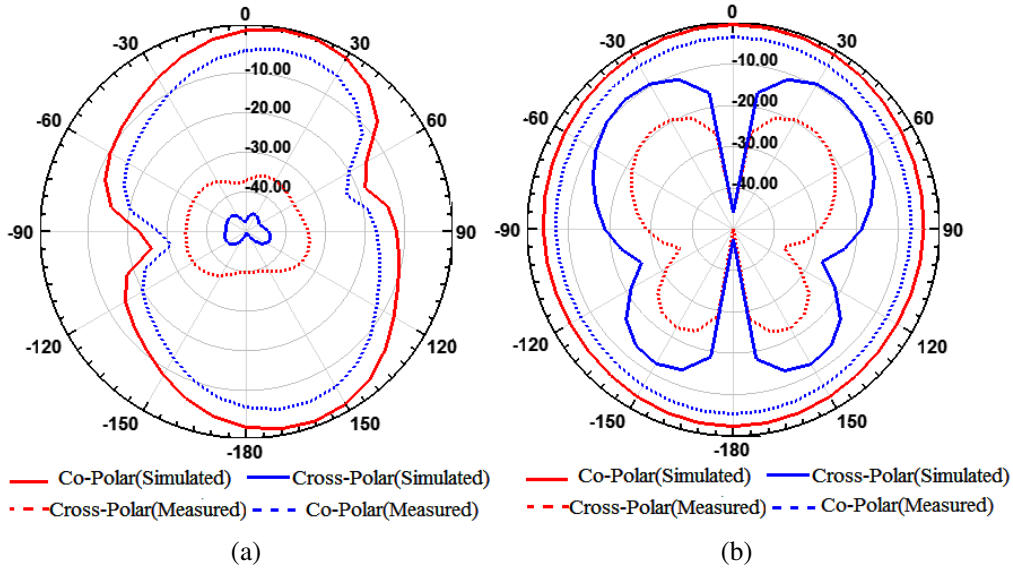


Figure 23. Radiation patterns at 9 GHz. (a) *E*-plane. (b) *H*-plane.

Table 2. Comparisons of compactness in conventional and DG-CEBG structures.

Notch Frequency	Mushroom EBG structure size	Defected Ground Compact EBG structure (DG-CEBG) size	Percentage Compactness Achieved
WiMAX Band	9.25 mm	5 mm	45.9%
WLAN Band	6.1 mm	3 mm	50.0%
7.2–8.4 GHz Band	3.3 mm	1.7 mm	48.5%

UWB frequency range of 3.1–10.6 GHz. The calculated value of ECC is low, and hence it can give good diversity performance for UWB MIMO systems. The ECC is less than 0.5 and within the acceptable limits, which ensures acceptable behavior of the proposed UWB/MIMO antenna over the whole UWB frequency range. Table 2 indicates a comparison of the size reduction in mushroom and DG-CEBG structures. WiMAX, WLAN, and the 7.2–8.4 GHz band DG-CEBG structures show size reductions of 45.9%, 50.0%, and 48.4%, respectively. Table 3 shows the different techniques available in literature to obtain notches. DG-CEBG structures can be used with most of the antenna shapes to obtain notches without modifying the antenna design.

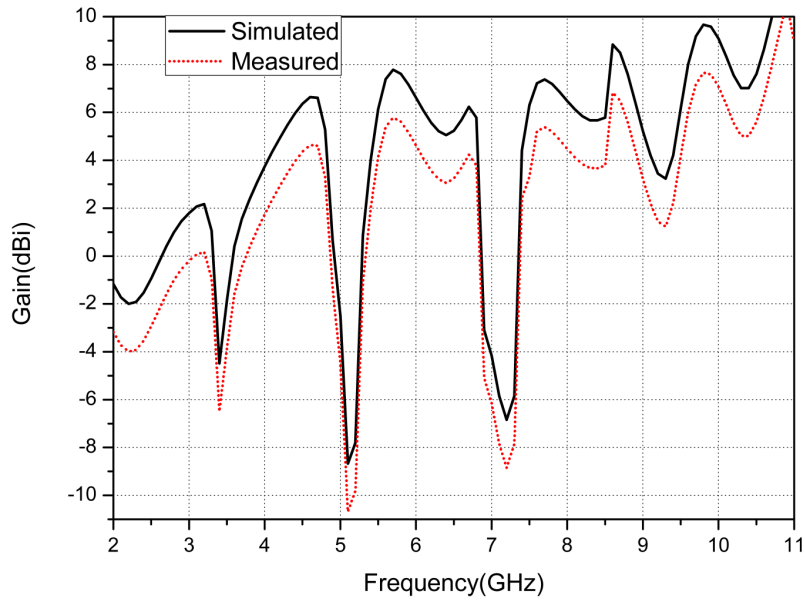


Figure 24. Antenna gain variation with frequency.

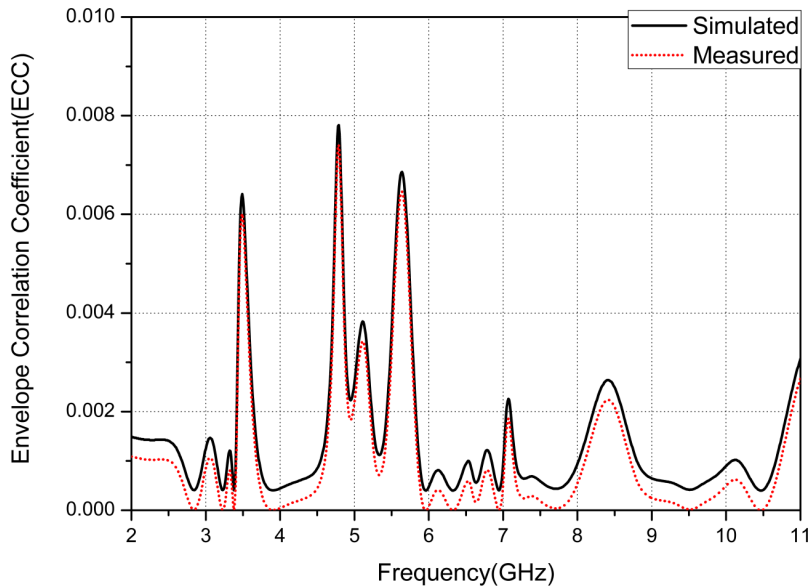


Figure 25. Simulated and measured ECC variation with frequency.

Table 3. Comparisons of different techniques available to obtain notches.

Reference	No. of Radiating Elements	Notch Techniques	Notched frequencies (GHz)
[20]	1	Four EBG structures	5.15–5.95
[21]	1	Two EBG structures	4.98–5.43 & 5.64–5.93
[41]	2	Split ring resonators	WLAN Band
[59]	2	Strips in antenna ground	5.15–5.85
[60]	2	L-type Stubs	3.62–4.77
[61]	2	Slit in the radiator	5.15–5.925
[62]	4	Band stop design and pin diode	5.15–5.825
[63]	4	Band stop design	5.15–5.825
[64]	4	Quarter wave stub and pin diode	4.8–6.2
Proposed	2	Five DG-CEBG structures	WiMAX, WLAN and X-band

6. CONCLUSION

In this article, a triple band rejection UWB MIMO/Diversity antenna with reduced wideband electromagnetic coupling among individual antenna elements is discussed. The proposed antenna is fabricated on a cheaply available FR-4 substrate with an overall size of $58 \times 45 \times 1.6 \text{ mm}^3$. A good impedance bandwidth from 3.1 GHz to 11 GHz has been achieved with triple notches at WiMAX band (3.3–3.6 GHz), WLAN band (5–6 GHz), and X-band satellite communication (7.2–8.4 GHz) band. The mutual coupling among individual antennas in both simulated and measured results is below 15 dB. This value is sufficient for most of the MIMO/Diversity applications across the whole UWB band. The values of ECC are at an acceptable limit that ensures good performance of the proposed antenna. There is a good consistency between measured and simulated results.

REFERENCES

1. Federal Communications Commission, “Revision of part 15 of the commission’s rules regarding ultra-wideband transmission systems,” Tech. Rep. ET-Docket 98-153, FCC02-48, Federal Communications Commission (FCC), Washington, DC, USA, 2002.
2. Liang, J., C. C. Chiau, X. Chen, and C. G. Parini, “Printed circular disc monopole antenna for ultra-wideband applications,” *Electron. Lett.*, Vol. 40, No. 20, 1246–1248, 2004
3. Sarkar, D., K. Sarkar, and K. Saurav, “A compact microstrip-fed triple band-notched UWB monopole antenna,” *IEEE Antennas and Wireless Propagation Letters*, Vol. 13, 396–399, Feb. 2014.
4. Zhu, F., S. Gao, A. T. S. Ho, A. Al Hameed, C. H. See, T. W. C. Brown, J. Li, G. Wei, and J. Xu, “Multiple band-notched UWB antenna with band-rejected elements integrated in the feed line,” *IEEE Transactions on Antennas and Propagation*, Vol. 61, No. 5, 3952–3960, 2013.
5. Foudazi, A., H. R. Hassani, and S. M. Ali Nezhad, “Small UWB planar monopole antenna with added GPS/GSM/WLAN bands,” *IEEE Transactions on Antennas and Propagation*, Vol. 60, No. 6, 2987–2992, 2012.
6. Li, W. T., X. W. Shi, and Y. Q. Hei, “Novel planar UWB monopole antenna with triple band-notched characteristics,” *IEEE Antennas and Wireless Propagation Letters*, Vol. 8, 1094–1098, 2009.

7. Nguyen, D. T., D. H. Lee, and H. C. Park, "Very compact printed triple band-notched UWB antenna with quarter-wavelength slots," *IEEE Antennas and Wireless Propagation Letters*, Vol. 11, 411–414, 2012.
8. Trang, N. D., D. H. Lee, and H. C. Park, "Design and analysis of compact printed triple band-notched UWB antenna," *IEEE Antennas and Wireless Propagation Letters*, Vol. 10, 403–406, 2011.
9. Almalkawi, M. and V. Devabhaktuni, "Ultrawideband antenna with triple band-notched characteristics using closed-loop ring resonators," *IEEE Antennas and Wireless Propagation Letters*, 959–962, 2011.
10. Tang, M. C., S. Xiao, T. Deng, D. Wang, J. Guan, B. Wang, and G. D. Ge, "Compact UWB antenna with multiple band-notches for WiMAX and WLAN," *IEEE Transactions on Antennas and Propagation*, Vol. 59, No. 4, 1372–1376, 2011.
11. Deng, J. Y., Y. Z. Yin, S. G. Zhou, and Q. Z. Liu, "Compact ultra-wideband antenna with tri-band notched characteristics," *Electron. Lett.*, Vol. 44, No. 21, 1231–123, 2008.
12. Mohammadian, N., M. N. Azarmanesh, and S. Soltani, "Compact ultra-wideband slot antenna fed by coplanar waveguide and microstrip line with triple-band-notched frequency function," *IET Microw., Antennas Propag.*, Vol. 4, No. 11, 1811–1817, 2010.
13. Vendik, I. B., A. Rusakov, K. Kanjanasit, J. Hong, and D. Filonov, "Ultrawideband (UWB) planar antenna with single-, Dual-, and triple-band notched characteristic based on ring resonator," *IEEE Antennas and Wireless Propagation Letters*, Vol. 16, 1597–1600, 2017.
14. Liu, Y., Z. Chen, and S. Gong, "Triple band-notched aperture UWB antenna using hollow-cross-loop resonator," *Electron. Lett.*, Vol. 50, No. 10, 728–730, May 2014.
15. Mohammed, H. J., et al., "Design of a uniplanar printed triple band-rejected ultra-wideband antenna using particle swarm optimisation and the fire-fly algorithm," *IET Microw., Antennas Propag.*, Vol. 10, No. 1, 31–37, Jan. 2016.
16. Cai, Y. Z., H. C. Yang, and L. Y. Cai, "Wideband monopole antenna with three band-notched characteristics," *IEEE Antennas and Wireless Propagation Letters*, Vol. 13, 607–610, 2014.
17. Ali, W. A. E. and R. M. A. Moniem, "Frequency reconfigurable triple band-notched ultra-wideband antenna with compact size," *Progress in Electromagnetics Research C*, Vol. 73, 37–46, 2017.
18. Abdelhalim, C. and D. Farid, "A compact planar UWB antenna with triple controllable band notched characteristics," *International Journal of Antennas and Propagation*, Vol. 2014, 10 pages, Article ID 848062, 2014.
19. Wang, Q. and Y. Zhang, "Design of a compact UWB antenna with triple band-notched characteristics," *International Journal of Antennas and Propagation*, Vol. 2014, 9 pages, Article ID 892765, 2014.
20. Yazdi, M. and N. Komjani, "Design of a band-notched UWB monopole antenna by means of an EBG structure" *IEEE Transactions on Antennas and Wireless Propagation*, Vol. 10, 170–173, Jan. 2011.
21. Peng, L. and C. Ruan, "UWB band-notched monopole antenna design using electromagnetic-bandgap structures," *IEEE Transactions on Microwave Theory and Techniques*, Vol. 59, 1074–1081, Apr. 2011.
22. Jensen, M. A. and J. W. Wallace, "A review of antennas and propagation for MIMO wireless communication," *IEEE Transactions on Antennas and Propagation*, Vol. 52, No. 11, 2810–2824, Nov. 2004.
23. Song, Y., T. N. Guo, R. C. Qiu, and M. C. Wicks, "A real time UWB MIMO system with programmable transmit waveforms: Architecture, algorithms and demonstrations," *IEEE Transactions on Antennas and Propagation*, Vol. 60, No. 8, 3933–3940, Aug. 2012.
24. Song, Y., N. Guo, and R. C. Qiu, "Implementation of UWB MIMO time-reversal radio testbed," *IEEE Antennas and Wireless Propagation Letters*, Vol. 10, 796–799, 2011.
25. Ben, I. M., L. Talbi, M. Nedil, and K. Hettak, "MIMO-UWB channel characterization within an underground mine gallery," *IEEE Transactions on Antennas and Propagation*, Vol. 60, No. 10, 4866–4874, Oct. 2012.

26. Lu, S., T. Hui, and M. Bialkowski, "Optimizing MIMO channel capacities under the influence of antenna mutual coupling," *IEEE Antennas and Wireless Propagation Letters*, Vol. 7, 287–290, Jul. 2008.
27. Fletcher, P. N., M. Dean, and A. R. Nix, "Mutual coupling in multi element array antennas and its influence on MIMO channel capacity," *Electron. Lett.*, Vol. 39, No. 4, 342–344, Feb. 2003.
28. Chiau, C. C., X. Chen, and C. G. Parini, "A miniature dielectric-loaded folded half-loop antenna and ground plane effects," *IEEE Antennas and Wireless Propagation Letters*, Vol. 4, No. 1, 459–462, Dec. 2005.
29. Gao, Y., X. Chen, Z. Ying, and C. Parini, "Design and performance investigation of a dual-element PIFA array at 2.5 GHz for MIMO terminal," *IEEE Transactions on Antennas and Propagation*, Vol. 55, No. 12, 3433–3441, Dec. 2007.
30. Chiu, C.-Y., C.-H. Cheng, R. D. Murch, and C. R. Rowell, "Reduction of mutual coupling between closely packed antenna elements," *IEEE Transactions on Antennas and Propagation*, Vol. 55, No. 6, 1732–1738, Jun. 2007.
31. Kokkinos, T., E. Liakou, and A. P. Feresidis, "Decoupling antenna elements of PIFA arrays on handheld devices," *IET Electronic Letters*, Vol. 44, No. 25, 1442–1444, 2008.
32. Karaboikis, M., C. Soras, G. Tsachtsiris, and V. Makios, "Compact dual-printed inverted-F antenna diversity systems for portable wireless devices," *IEEE Antennas and Wireless Propagation Letters*, Vol. 3, No. 1, 9–14, Dec. 2004.
33. Yang, F. and Y. Rahmat-Samii, "Microstrip antennas integrated with electromagnetic band-gap (EBG) structures: A low mutual coupling design for array applications," *IEEE Transactions on Antennas and Propagation*, Vol. 51, No. 10, 2936–2946, Oct. 2003.
34. Rajo-Iglesias, E., O. Quevedo-Teruel, and L. Inclan-Sanchez, "Mutual coupling reduction in patch antenna arrays by using a planar EBG structure and a multilayer dielectric substrate," *IEEE Transactions on Antennas and Propagation*, Vol. 56, No. 6, 1648–1655, Jun. 2008.
35. See, T. S. P. and Z. N. Chen, "An ultra wideband diversity antenna," *IEEE Transactions on Antennas and Propagation*, Vol. 57, No. 6, 1597–1605, 2009.
36. Rajagopalan, A., G. Gupta, A. S. Konanur, B. Hughes, and G. Lazzi, "Increasing channel capacity of an ultrawideband MIMO system using vector antennas," *IEEE Transactions on Antennas and Propagation*, Vol. 55, No. 10, 2880–2887, 2007.
37. Zhang, S., B. K. Lau, A. Sunesson, and S. He, "Closely-packed UWB MIMO/diversity antenna with different patterns and polarizations for USB dongle applications," *IEEE Transactions on Antennas and Propagation*, Vol. 60, No. 9, 4372–4380, 2012.
38. Yoon, H. K., Y. J. Yoon, H. Kim, and C. H. Lee, "Flexible ultra-wideband polarization diversity antenna with band-notch function," *IET Microw. Antennas Propag.*, Vol. 5, No. 12, 1463–1470, Sep. 2011.
39. Lee, J. M., K. B. Kim, H. K. Ryu, and J. M. Woo, "A compact ultrawideband MIMO antenna with WLAN band-rejected operation for mobile devices," *IEEE Antennas and Wireless Propagation Letters*, Vol. 11, 990–993, Aug. 2012.
40. Li, J. F., Q. X. Chu, Z. H. Li, and X. X. Xia, "Compact dual band-notched UWB MIMO antenna with high isolation," *IEEE Transactions on Antennas and Propagation*, Vol. 61, No. 9, 4759–4766, Sep. 2013.
41. Gao, P. et al., "Compact printed UWB diversity slot antenna with 5.5-GHz band-notched characteristics," *IEEE Antennas and Wireless Propagation Letters*, Vol. 13, 376–379, Feb. 2014.
42. Chacko, B. P., G. Augustin, and T. A. Denidni, "Uniplanar polarization diversity antenna for wideband systems," *IET Microw. Antennas Propag.*, Vol. 7, No. 10, 851–857, Jul. 2013.
43. Li, J. F., D. L. Wu, and Y. J. Wu, "Dual band-notched UWB MIMO antenna with uniform rejection performance" *Progress In Electromagnetics Research M*, Vol. 54, 103–111, 2017.
44. Toktas, A., "G-shaped band-notched ultra-wideband MIMO antenna system for mobile terminals," *IET Microw., Antennas Propag.*, Vol. 11, No. 5, 718–725, 2017.
45. Liu, L., S. W. Cheung, and T. I. Yuk, "Compact MIMO antenna for portable UWB applications

- with band-notched characteristic," *IEEE Transactions on Antennas and Propagation*, Vol. 63, No. 5, 1917–1924, 2015.
46. Sievenpiper, D., "High-impedance electromagnetic surfaces," Ph.D. dissertation, Department of Electrical Engineering University of California, Los Angeles, CA, 1999.
 47. Yang, F. and Y. Rahmat-Samii, *Electromagnetic Band Gap Structures in Antenna Engineering*, Cambridge University Press, 2009.
 48. Jaglan, N., S. D. Gupta, B. K. Kanaujia, and S. Srivastava, "Band notched UWB circular monopole antenna with inductance enhanced modified mushroom EBG structure," *Wireless Networks, Springer*, Aug. 1–11, 2016, DOI: 10.1007/s11276-016-1343-7.
 49. Jaglan, N., B. K. Kanaujia, S. D. Gupta, and S. Srivastava, "Triple band notched UWB antenna design using electromagnetic band gap structures," *Progress In Electromagnetics Research C*, Vol. 66, 139–147, Jul. 2016.
 50. Sohn, J. R., K. Y. Kim, H.-S. Tae, and H. J. Lee, "Comparative study on various artificial magnetic conductors for low-profile antenna," *Progress In Electromagnetics Research*, Vol. 61, 27–37, 2006.
 51. Jaglan, N., S. D. Gupta, B. K. Kanaujia, and S. Srivastava, "Design and development of efficient EBG structures based band notched UWB circular monopole antenna," *Wireless Personal Communication*, 1–27, Springer, May 2017, DOI: 10.1007/s11277-017-4446-2.
 52. Ahmed, O. and A. R. Sebak, "A printed monopole antenna with two steps and a circular slot for UWB applications," *IEEE Antennas and Wireless Propagation Letters*, Vol. 7, 411–413, 2008.
 53. Assimonis, S. D., T. V. Yioultsis, and C. S. Antonopoulos, "Design and optimization of uniplanar EBG structures for low profile antenna applications and mutual coupling reduction," *IEEE Transactions on Antennas and Propagation*, Vol. 60, No. 10, 4944–4949, Oct. 2012.
 54. Mu, X., W. Jiang, S.-X. Gong, and F.-W. Wang, "Dual-band low profile directional antenna with high impedance surface reflector," *Progress In Electromagnetics Research Letters*, Vol. 25, 67–75, 2011.
 55. Saraswat, R. K. and M. Kumar, "A frequency band reconfigurable UWB antenna for high gain applications," *Progress In Electromagnetics Research B*, Vol. 64, 29–45, 2015.
 56. Saraswat, R. K. and M. Kumar, "Miniaturized slotted ground UWB antenna loaded with metamaterial for WLAN and WiMAX applications," *Progress In Electromagnetics Research B*, Vol. 65, 65–80, 2016.
 57. Blanch, S., J. Romeu, and I. Corbella, "Exact representation of antenna system diversity performance from input parameter description," *Electron. Lett.*, Vol. 39, No. 9, 705–707, May 2003.
 58. Srivastava, G. and A. Mohan, "Compact MIMO slot antenna for UWB applications," *IEEE Antennas and Wireless Propagation Letters*, Vol. 15, 1057–1060, 2015.
 59. Kang, L., H. Li, et al., "Compact offset microstrip-fed MIMO antenna for band-notched UWB application," *IEEE Antennas and Wireless Propagation Letters*, Vol. 14, 1754–1757, 2015.
 60. Chandel, R. and A. K. Gautam, "Compact MIMO/diversity slot antenna for UWB applications with band-notched characteristics," *Electron. Lett.*, Vol. 52, 336–338, 2016.
 61. Zhu, J., S. Li, et al., "Compact dual polarized UWB quasi-self-complementary MIMO/diversity antenna with band rejection capability," *IEEE Antennas and Wireless Propagation Letters*, Vol. 15, 905–908, 2015.
 62. Khan, M. S., A. Iftikhar, S. Asif, A.-D. Capobianco, and B. D. Braaten, "A compact four elements UWB MIMO antenna with on-demand WLAN rejection," *Microwave and Optical Technology Letters*, Vol. 58, No. 2, 270–276, Feb. 2016.
 63. Khan, M. S., A. D. Capobianco, S. Asif, A. Iftikhar, B. Ijaz, and B. D. Braaten, "Compact 4×4 UWB-MIMO antenna with WLAN band rejected operation," *IET Electronic Letters*, Vol. 51, No. 14, 1048–1050, Jul. 2015.
 64. Khan, M. S., A.-D. Capobianco, A. Naqvi, M. F. Shafique, B. Ijaz, and B. D. Braaten, "Compact planar UWB MIMO antenna with on-demand WLAN rejection," *IET Electronic Letters*, Vol. 51, No. 13, 963–964, Jun. 2015.

Erratum to “Triple Band Notched DG-CEBG Structure Based UWB MIMO/Diversity Antenna” by Naveen Jaglan, Samir D. Gupta, Binod K. Kanaujia, Shweta Srivastava, and Ekta Thakur
in Progress In Electromagnetics Research C, Vol. 80, 21–37, 2018

**Naveen Jaglan^{1, 2, *}, Samir D. Gupta¹, Binod K. Kanaujia³,
Shweta Srivastava¹, and Ekta Thakur²**

The authors want to add one more reference paper that may help in antenna design:

Kharche, S., G. S. Reddy, R. K. Gupta, and J. Mukherjee, “MIMO antenna for bluetooth, Wi-Fi, Wi-MAX and UWB applications,” *Progress In Electromagnetics Research PIER C*, Vol. 52, 53–62, 2014.

The authors apologize for this error.

Received 20 June 2018, Added 20 June 2018

* Corresponding author: Naveen Jaglan (naveenjaglan1@gmail.com).

¹ Department of Electronics & Communication Engineering, Jaypee Institute of Information Technology, Noida, Uttar Pradesh, India. ² Department of Electronics & Communication Engineering, Jaypee University of Information Technology, Waknaghat, Solan, Himachal Pradesh, India. ³ School of Computational & Integrative Sciences, Jawaharlal Nehru University (J.N.U.), New Delhi 110067, India.